Light-gated binding in double-motorized porphyrin cages

Roeland Nolte[1], Pieter Gilissen[1], Nicolas Vanthuyne[2], Ben Feringa[3], and Johannes Elemans[4]

[1]Radboud University
[2]Aix Marseille Univ, CNRS, Centrale Marseille, iSm2, Marseille, France
[3]Groningen University Faculty of Mathematics and Natural Sciences
[4]Radboud Universiteit Nijmegen

August 9, 2021

Abstract

Molecular motors change conformation under the influence of light and when attached to host molecules they may find applications as sensors and switchable catalysts. Here we present a porphyrin macrocyclic host functionalized with two motor appendages for future catalytic applications. The compound is formed as a mixture of six stereoisomers (three sets of enantiomers), which have been separated by (chiral) chromatography. 1H NMR and chiral spectroscopy revealed that in one set of diastereomers the two motors interact with the cavity of the host (bound-bound), whereas in a second set one interacts and the other one does not (bound-loose). In the third set both motors do not interact with the host compound (loose-loose). The motorized hosts bind guest molecules in the order: (loose-loose) > (bound-loose) > (bound-bound). They can be switched with light to pseudo-identical diastereomers, leading to orthogonal behavior in the light-gated binding of guest molecules. Whereas the photo-isomerization of the diastereomer set loose-loose significantly lowers the binding affinity for viologen guests, the opposite is true for the diastereomer set bound-bound, i.e. the binding affinity increases. For the diastereomer set bound-loose no influence on guest binding is observed as the effect of photoisomerization on the motors is cancelled out.

Pieter J. Gilissen,[1] Nicolas Vanthuyne,[2] Ben L. Feringa,[3,*] Johannes A.A.W. Elemans,[1,*] and Roeland J.M. Nolte[1,*]

[1]Radboud University, Institute for Molecules and Materials, Heyendaalseweg 135, 6525 AJ Nijmegen, the Netherlands

[2]Aix Marseille Univ, CNRS, Centrale Marseille, iSm2, Marseille, France. [3]University of Groningen, Stratingh Institute for Chemistry, Nijenborgh 4, 9747 AG Groningen, the Netherlands

Correspondence

Johannes A.A.A.W. Elemans and Roeland J.M. Nolte, Radboud University, Institute for Molecules and Materials, Heyendaalseweg 135, 6525 AJ Nijmegen, the Netherlands,

Ben L. Feringa, University of Groningen, Stratingh Institute for Chemistry, Nijenborgh 4, 9747 AG Groningen, the Netherlands

E-mail:

r.nolte@science.ru.nl**; j.elemans@science.ru.nl; b.l.feringa@rug.nl**

Funding information

European Research Council grants (ERC Advanced Grant No. 74092 to R.J.M.N. and ERC Advanced Grant No. 227897 to B.L.F.); Dutch Ministry of Education, Culture, and Science grant (Gravitation program 024.001.035).

Abstract: Molecular motors change conformation under the influence of light and when attached to host molecules they may find applications as sensors and switchable catalysts. Here we present a porphyrin macrocyclic host functionalized with two motor appendages for future catalytic applications. The compound is formed as a mixture of six stereoisomers (three sets of enantiomers), which have been separated by (chiral) chromatography. ^{1}H NMR and chiral spectroscopy revealed that in one set of diastereomers the two motors interact with the cavity of the host (*bound-bound*), whereas in a second set one interacts and the other one does not (*bound-loose*). In the third set both motors do not interact with the host compound (*loose-loose*). The motorized hosts bind guest molecules in the order: (*loose-loose*) > (*bound-loose*) > (*bound-bound*). They can be switched with light to pseudo-identical diastereomers, leading to orthogonal behavior in the light-gated binding of guest molecules. Whereas the photo-isomerization of the diastereomer set*loose-loose* significantly lowers the binding affinity for viologen guests, the opposite is true for the diastereomer set*bound-bound* , i.e. the binding affinity increases. For the diastereomer set *bound-loose* no influence on guest binding is observed as the effect of photoisomerization on the motors is cancelled out.

Stimuli-responsive host-guest systems mimic the dynamic and regulatory behavior of enzyme-substrate complexes and various examples of such artificial systems have been published in the past.[1–6] A frequently used non-invasive stimulus is light,[2] which can activate a chromophore present in the host or the guest leading to a change in the electronic or three-dimensional structure of these molecules and hence a change in their affinity. Photo-responsive macrocyclic hosts based on various chromophores have been described in the literature, including azobenzenes, stilbenes, and dithienylethenes. While azobenzenes[7] and stilbenes[8] undergo photochemical *E* -*Z* isomerizations, dithienylethenes[9] are involved in photochemical cyclizations and ring-openings. Various host molecules, e.g. cyclodextrins, have been equipped with photo-switches in order to tune their binding properties.[10,11] In addition, an artificial muscle was developed employing cyclodextrins in combination with azobenzene-functionalized polymeric guest molecules.[12] Other extensively studied hosts are crown ethers, which have been connected to azobenzene[13] and stilbene photoswitches,[14,15] for photo-switchable guest binding and on/off-catalysis. Azobenzene-functionalized cationic guests have been used for light-powered threading through crown ethers.[16] More recently, a molecular motor-functionalized crown ether was developed,[17] in which host-guest interactions were used to tune specific properties of the molecular motor, *i.e.* the rotation rate and the photostationary state. In addition, molecular motors capable of tuning the chiral environment of the crown ether host, allowing enantio-divergent binding and recognition of chiral guests have been reported.[18,19] Molecular motors offer the unique property of photochemically induced helical inversion,[20,21] which allowed for the construction of photo-switchable asymmetric catalysts.[22,23]

In our group, we have developed a porphyrin macrocyclic host (*i.e.* cage compound **Zn1** , Figure 1),[24]consisting of a glycoluril framework that is connected to a porphyrin roof via xylylene side walls and crown ether-like linkages. **Zn1**is an excellent host for viologen guests, which are bound in the cavity of **Zn1** by a combination of electrostatic and π-stacking effects.[24] As part of a program aimed at the development of a supramolecular catalytic system that can write information on a polymeric thread we recently reported on the synthesis and properties of molecular motor-functionalized porphyrin cage**Zn2** ,[25] which combines the rotational properties of a free molecular motor with the host-guest binding properties of the parent porphyrin cage **Zn1** . Since **Zn2**contains only one motor substituent the two faces of the cavity of this porphyrin host are non-identical, causing ambiguity in the binding and threading process of guest molecules. Here we report the synthesis and physical properties of a porphyrin cage (**Zn3**), of which both faces of the molecule are equipped with a motor function, eliminating this ambivalence. Host molecule **Zn3** possesses three distinct stereochemical elements, *i.e.* point chirality at the four chiral centers, planar chirality resulting from the presence of substituents on the xylylene sidewalls,[26] and axial chirality on both molecular motor substituents. The combination of fixed planar chirality and photo-switchable axial chirality (helicity) is exploited in the orthogonal dynamic binding of viologen guests.

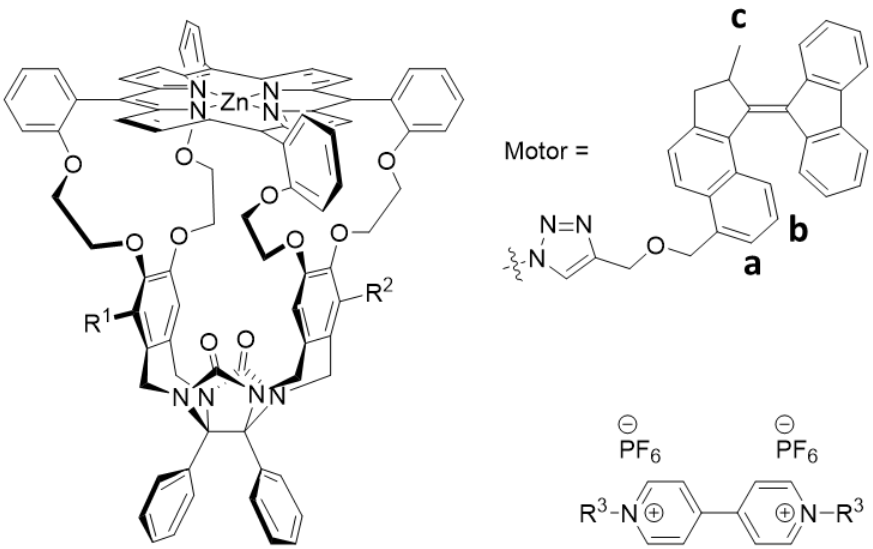

Zn1 (R^1 = R^2 = H)
Zn2 (R^1 = H, R^2 = Motor)
Zn3 (R^1 = R^2 = Motor)

V4 (R^3 = methyl)
V5 (R^3 = benzyl)
V6 (R^3 = *n*-pentyl)

FIGURE 1 Chemical structures of the host and guest molecules used in this study. For clarity, only the S_p isomers of the porphyrin cage compounds are depicted. See Supporting Information, Figure S13 for the chemical structures of all individual stereoisomers.

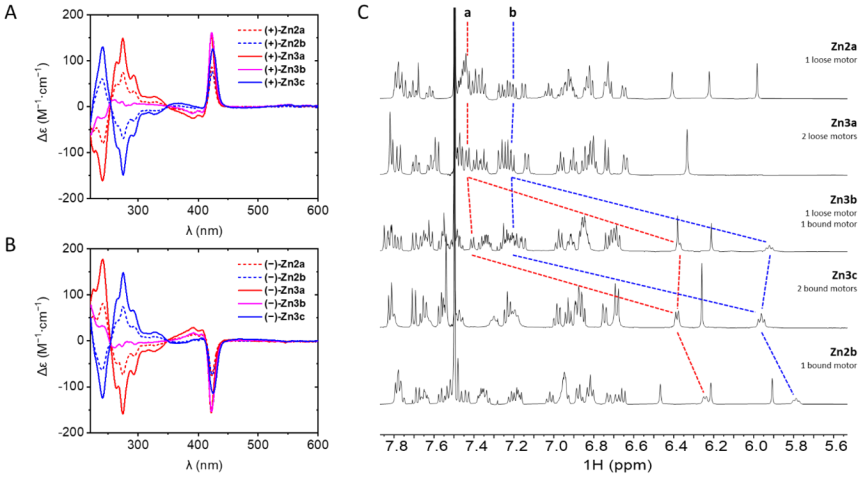

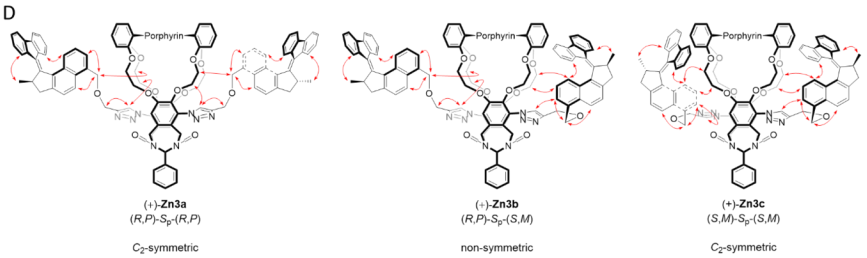

For the synthesis of the double-motorized porphyrin cage compound**Zn3** (Supporting Information, Scheme S1) we followed the same strategy as applied for the synthesis of mono-motorized cage**Zn2** .[25] Compound **Zn3** was obtained as a mixture of six stereoisomers, *i.e.* three diastereomeric sets of enantiomers. The different diastereomers **Zn3a** (first eluted, C_2-symmetric), **Zn3b** (second eluted, non-symmetric), and **Zn3c** (third eluted, C_2-symmetric), see Figure 2, were separated by conventional silica gel column chromatography. We resolved the enantiomers of each diastereomeric set in order to be able to obtain more information about the structures of the individual compounds by chiroptical spectroscopy. Resolution was achieved by preparative chiral HPLC using a Chiralpak IE column (Supporting Information, Figures S1–S12). The ECD spectra of all the enantiomers of double-motorized compound **Zn3** were compared to the ECD spectra of the corresponding single-motorized compound **Zn2** (Figure 2A–B), especially with respect to the Cotton effect of the molecular motor absorption band at 250–300 nm and the Cotton effect of the Soret band at 420–430 nm. Isomers with a positive Cotton effect of the Soret band were assigned (+), and those with a negative Cotton effect of the Soret band were assigned (-). The relative stereochemistry of **Zn3a**was identical to that of **Zn2a** , *i.e.* for both compounds the motor and Soret CD bands had the same sign. Compounds **Zn3c**and **Zn2b**also displayed similarities, in the sense that the motor and Soret CD bands had opposite signs. Because

FIGURE 2 Spectroscopic comparison of motorized porphyrin cage compounds**Zn2** and **Zn3** . ECD spectra (CH_2Cl_2, 298 K) of: (A) (+)-**Zn2**and (+)-**Zn3** ; (B) (-)-**Zn2** and (-)-**Zn3** . (C) Partial ^{1}H NMR spectra (500 MHz, $CDCl_3/CD_3CN$, 1:1, v/v, 298 K) of**Zn2** and **Zn3** . See Figure 1 for the proton assignments. (D) Key NOEs (red arrows) of motor protons, spatial orientation, and absolute configuration of isomers (+)-**Zn3a** , (+)-**Zn3b** , and (+)-**Zn3c** . The descriptors (R,P) and/or (S,M) represent the point chirality and helicity of the molecular motor substituents in their stable configuration, and the descriptor S_p (or R_p, not shown in this Figure) represents the planar chirality of the porphyrin cage.

of the presence of two motor substituents, the magnitude of the Cotton effect of the motor substituents of **Zn3a** and **Zn3c** was doubled with respect to that of **Zn2a** and **Zn2b** . The non-symmetric compound **Zn3b** is different from all the other compounds, since it contains two molecular motor substituents with opposite chirality and, therefore, the motor CD band was absent. Comparison of the CD spectra of **Zn3** with those of **Zn2**allowed the determination of the absolute configuration of each isomer (Supporting Information, Table S1). The ^{1}H NMR spectra of **Zn2** and **Zn3** gave additional evidence for the above-mentioned differences and similarities between the compounds (Figure 2C). In our previous work on single-motorized cage **Zn2**we showed that the chemical shifts of motor protons H-**a** and H-**b** were indicative of the presence or absence of intramolecular interactions between the naphthalene part of the motor and the cavity of the porphyrin cage.[25] The presence of such interactions in compound **Zn2b** was evidenced by a strong shielding effect on protons H-**a** and H-**b** , which is caused by the parallel displaced π-π stacking of the naphthalene part of the motor and the porphyrin. In contrast, this shielding effect was not present in **Zn2a** and also not in theC_2-symmetric compound **Zn3a** , confirming their similarity. It was observed, however, for one of the two motors of non-symmetric compound **Zn3b** , and for both motors ofC_2-symmetric compound **Zn3c** . These observations indicate similarities between the three-dimensional structures of single- and double-motorized porphyrin cages **Zn2**and **Zn3** . We conclude, therefore, that **Zn3a** contains two molecular motors, which both are loosely connected to the cage with no significant intramolecular interaction with the cage cavity. On the other hand, **Zn3b** is equipped with one 'loose' molecular motor, and one molecular motor that is intramolecularly 'bound' to the cavity. Finally, compound **Zn3c** carries two 'bound' molecular motors. 2D

ROESY experiments confirmed the three-dimensional structures of the different isomers of **Zn3** (Figure 2D). The differences in steric impediment between the 'loose' and 'bound' molecular motors may translate into different affinities of the cage compounds for guest molecules, *i.e.* it is expected that one or more 'bound' motor substituents will inhibit binding of a guest in the cavity of host**Zn3** .

We reported previously that porphyrin cage compounds**Zn1** [24] and **Zn2** [25]display a high affinity for viologen guests. In this study, we evaluated the binding affinities of the different isomers of **Zn3** for viologen guests **V4** –**V6** by fluorescence titrations (Table 1). During these titrations, the porphyrins were excited at their main Q-band ($\lambda_{ex} = 555$ nm) to avoid in situ excitation of the molecular motor substituents. The experiments revealed that isomer **Zn3a** (two loose motors) binds all viologen guests with a roughly two times higher association constant (K_a) than isomer **Zn3b** (one loose motor, one bound motor). In turn, isomer **Zn3b** binds the guests with a roughly two times higher K_a-value than isomer**Zn3c** (two bound motors). Apparently, bound motor substituent progressively impede the binding of the viologen guest. The absolute values of the association constants depend on the N -substituents of the viologen. We reason that for all isomers of **Zn3** the binding of n -pentyl viologen **V6** is more sterically demanding than the binding of methyl viologen **V4** , resulting in lower K_a-values. In contrast, benzyl viologen**V5** forms the strongest complexes with all the isomers of**Zn3** , which we attribute to the ability of the benzyl functions of this guest to form additional π-π interactions with the molecular motor substituents of the host. The binding studies and trends presented in Table 1 only represent the behavior of the motorized porphyrin cages in their stable ground states. Isomerization of the molecular motor substituents to the metastable states results in opposite relative stereochemistries, and therefore it may also result in different binding behavior.

TABLE 1 Association constants (K_a in M^{-1}) and Gibbs free energies (ΔG^0 in kJ/mol, in brackets) for the complexes of the isomers of porphyrin cage**Zn3** with viologen guests **V4** –**V6**($CHCl_3/CH_3CN$, 1:1, v/v, 298 K).

		Host	Host	Host	Relative association constant K_a
		Zn3a	**Zn3b**	**Zn3c**	**Zn3a** : **Zn3b** : **Zn3c**
Guest	**V4**	6.5×10^4 (-27.5)	3.7×10^4 (-26.1)	1.9×10^4 (-24.4)	3.4 : 1.9 : 1.0
	V5	3.0×10^5 (-31.5)	1.4×10^5 (-29.5)	6.3×10^4 (-27.4)	4.8 : 2.3 : 1.0
	V6	1.8×10^4 (-24.3)	8.7×10^3 (-22.5)	4.1×10^3 (-20.6)	4.3 : 2.1 : 1.0

Isomerization of a second-generation molecular motor (*e.g.***7** , Figure 3A) leads to helix inversion of the overcrowded alkene moiety.[21,27] The resulting metastable isomers are diastereomers of the stable isomers. The metastable isomer (R ,M)-**7-ms** is the pseudo-enantiomer of its corresponding stable isomer (R ,P)-**7-st** . These two isomers are called pseudo-enantiomers because they are near-mirror images, except for the methyl group at the stereogenic center. Metastable isomer (R ,M)-**7-ms** is pseudo-identical to the stable isomer (S ,M)-**7-st** . The term pseudo-identical, rather than identical, applies here because the point chirality at the motor stereogenic center differs between the

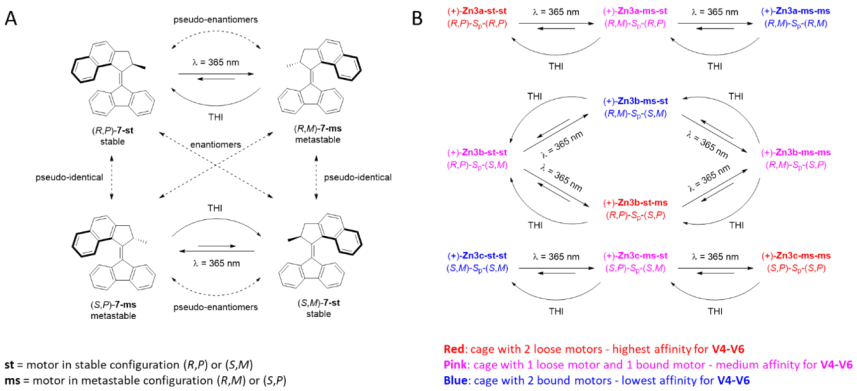

FIGURE 3 Isomerization pathways of: (A) molecular motor **7** , (B) the different isomers of double-motorized porphyrin cage **Zn3** . For clarity, only the pathways of the (+)-S_p isomers of the porphyrin cage compounds are depicted; the same mutual relationships are valid for the corresponding enantiomers with the (-)-R_p cage configuration.

pseudo-identical isomers. In the isomers of double-motorized cage compound **Zn3** , even more stereochemical elements are present than in **7** (Figure 3B). The planar chirality of the cage compound (R_p or S_p),[26] as well as the point chiralities at the stereogenic centers, (R) or (S), of the motor substituents are fixed. The only stereochemical element that can be isomerized is the helicity of the molecular motor (M or P), which is subject to photochemical inversion. Since the metastable isomer of a molecular motor is pseudo-identical to the stable isomer of the enantiomer of the same motor (Figure 3A), all the possible metastable isomers of any diastereomer of **Zn3** are pseudo-identical to the stable isomers of one of its other diastereomers. In Figure 3B all stable and metastable isomers of **Zn3** with the same color-code are considered to be pseudo-identical. In this more complex case, we call two isomers pseudo-identical if they possess identical motor helicities (M or P) and identical planar chiralities (R_p or S_p).

TABLE 2 Photochemical and thermal properties of single- and double-motorized porphyrin cages. UV-vis experiments were conducted in $CHCl_3/CH_3CN$ (1:1, v/v) and NMR experiments in $CDCl_3/CD_3CN$ (1:1, v/v). Values for **Zn2a** and **Zn2b** were taken from reference 25.

Compound	$t_{1/2}$ at 20 °C (UV-vis) (min)	$t_{1/2}$ at 20 °C (NMR) (min)	ΔG^{++} at 20 °C (kJ/mol)	PSS_{365} ratios at 4 °C (metastable : stable)
Zn2a[25]		11.6	88.6 ± 0.9	24 : 76
Zn2b[25]		5.3	86.7 ± 0.7	37 : 63
Zn3a	11.0	12.5	88.5 ± 1.5	25 : 75
Zn3b	6.8	9.7	87.3 ± 1.9	24 : 76
Zn3c	5.2	6.2	86.6 ± 0.3	23 : 77

UV-vis absorption spectroscopy was used to monitor the isomerization processes for the three different diastereomers of **Zn3** (Figure 4A–C). Irradiation of solutions containing either one of the isomers of **Zn3** with UV light (λ_{max} = 365 nm) to the photostationary state (PSS) resulted in an increase in absorption around λ = 460 nm, and a concomitant decrease in absorption around λ = 380 nm. The thermal helix inversion (THI) of the metastable motors to the stable motors restored the original UV-vis spectra. The processes of photochemical isomerization and subsequent thermal helix inversion were monitored at five different temperatures. The Eyring equation was used to determine the activation parameters for the thermal helix inversion steps (Table 2, Supporting Information, Figure S39, Table S20). UV-vis absorption spectroscopy

did not allow the determination of the rate constants for the THI step of each individual motor moiety attached to the host, *i.e.* the reported k_{THI}-values are apparent values (See Supporting Information, Equations 7–38). Nevertheless, double-motorized isomers **Zn3a** (two loose motors) and **Zn3c** (two bound motors) rotate with similar rates as the corresponding single-motorized isomers **Zn2a** (one loose motor) and **Zn2b** (one bound motor), respectively. Furthermore, the apparent rotation rate of the non-symmetric isomer **Zn3b** is in between the rotation rates of the other two diastereomers **Zn3a**and **Zn3c** . UV-vis absorption spectroscopy

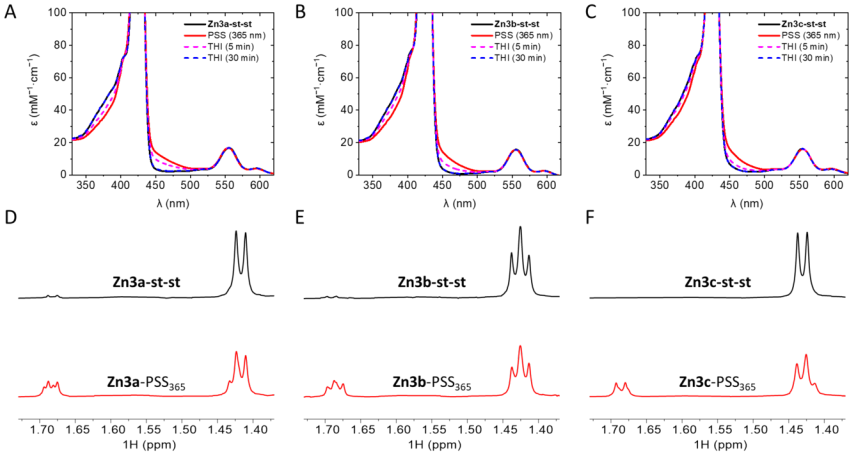

FIGURE 4 UV-vis spectra ($CHCl_3/CH_3CN$, 1:1, v/v, 298 K) of: (A) **Zn3a** , (B) **Zn3b** , and (C)**Zn3c** before irradiation (black), after irradiation to PSS_{365} (red), after partial THI (pink dashed), and after full THI (blue dashed). Partial ^{1}H NMR spectra (500 MHz, $CDCl_3/CD_3CN$, 1:1, v/v, 277 K) of: (D) **Zn3a** , (E) **Zn3b** , and (F) **Zn3c** before irradiation (black) and after irradiation to PSS_{365}(red) showing the signals of methyl protons H-**c** . See Figure 1 for the proton assignment. Note that the apparent triplet observed for the methyl protons of **Zn3b-st-st** is the result of two overlapping doublets originating from the two non-identical molecular motor substituents.

did not provide information about the relative abundance of the metastable and stable species in solution. In order to measure these PSS ratios, we resided to ^{1}H NMR spectroscopy (Figure 4D–F). The isomerization of the motor substituents of all isomers of**Zn3** with UV light (λ_{max} = 365 nm) resulted in similar deshieldings of the methyl protons H-**c** ($\Delta\delta$ = +0.26 ppm). After the subsequent thermal helix inversion, the original^{1}H NMR spectra were restored. The decays of the metastable states were determined by monitoring the signals of methyl protons H-**c** (Supporting Information, Figures S41–S44) over time, and the corresponding apparent rate constants were in reasonable agreement with those obtained by UV-vis spectroscopy (Table 2, second and third column). NMR spectroscopy was also used to probe the structural changes, as proposed in Figure 3B. The irradiation of**Zn3a** (two loose motors) resulted in metastable species with one or two bound motors ($\Delta\delta$ = -0.91 ppm for H-**a** , and $\Delta\delta$ = -0.84 ppm for H-**b**). As expected, the opposite effect was observed when**Zn3c** (two bound motors) was irradiated: new signals for loose motors ($\Delta\delta$ = +0.84 ppm for H-**a** , and $\Delta\delta$ = +1.24 ppm for H-**b**) were observed. For **Zn3b** , the situation was more complex, because of the absence of symmetry in the stable isomer and each of its three possible metastable isomers. Nevertheless, by monitoring the chemical shift changes of the aromatic protons attached to the xylylene sidewalls of the porphyrin cages, we could detect all proposed isomers (Supporting Information, Figures S49–S51). Moreover,^{1}H NMR analysis enabled us to determine the PSS ratios for the different diastereomers, *i.e.* the ratios between the total amount of metastable and stable motors (Table 2). These appeared to be nearly identical (metastable:stable ˜1:3) for all investigated double-motorized cages **Zn3** and also comparable to those found for the single-motorized cages **Zn2** . It has to be noted though that the measured PSS ratios, which are relatively low, cannot be considered to be accurate PSS ratios. In order to avoid aggregation

and precipitation of the porphyrin cages, the measurements were performed at 4 °C. At this temperature, the photochemical isomerization is still in competition with the thermal helix inversion. Lower temperatures would tackle this issue, but could not be applied as it results in precipitation of the porphyrin cages.

The differences in 3D structure between the stable isomers of**Zn3a** , **Zn3b** , and **Zn3c** caused significant differences in their binding affinities for viologen guests (**Zn3a** > **Zn3b** >**Zn3c** , see Table 1). These 3D structures could be changed by photochemical isomerization of the motor substituents (Figure 3). For instance, the stepwise isomerization of **Zn3a-st-st** (two loose motors) gives **Zn3a-ms-st** (one loose motor, one bound motor), and eventually **Zn3a-ms-ms** (two bound motors). The latter two isomers are pseudo-identical to **Zn3b-st-st** and**Zn3c-st-st** , respectively, both of which have a lower affinity for viologen guests. Therefore, we expected that the photochemical isomerization of **Zn3a-st-st** would also result in a stepwise lower binding affinity for viologen guests. Similarly, the stepwise isomerization of **Zn3c-st-st** to metastable isomers that are pseudo-identical to **Zn3b-st-st** and **Zn3a-st-st** should lead to an increase in the binding affinity for viologen guests. For the non-symmetric isomer **Zn3b-st-st** , photochemical isomerization to the mixture of metastable isomers is expected to have a minor influence on the binding affinity for viologen guests, as the isomerization effects of the two motor substituents would cancel out. We studied the light-gated binding of viologen guests **V4** –**V6** in the double-motorized porphyrin cages **Zn3** with the help of time-resolved fluorescence quenching spectroscopy (Figure 5). The host-guest complexes are non-fluorescent, and therefore the normalized fluorescence intensity originating from the zinc porphyrin after addition of guest is a measure for the amount of free host present in solution relative to the initial amount of free host. A normalized fluorescence intensity of 0.5 resembles a 1:1 mixture of free host and host-guest complex (50% occupancy). Based on the binding constants (Table 1), we calculated the amount of each guest that should be added to **Zn3b** (medium affinity for **V4** –**V6**) in order to reach ˜50% occupancy with an initial host concentration of 10^{-5} M (Supporting Information, Table S13). We first investigated the possible

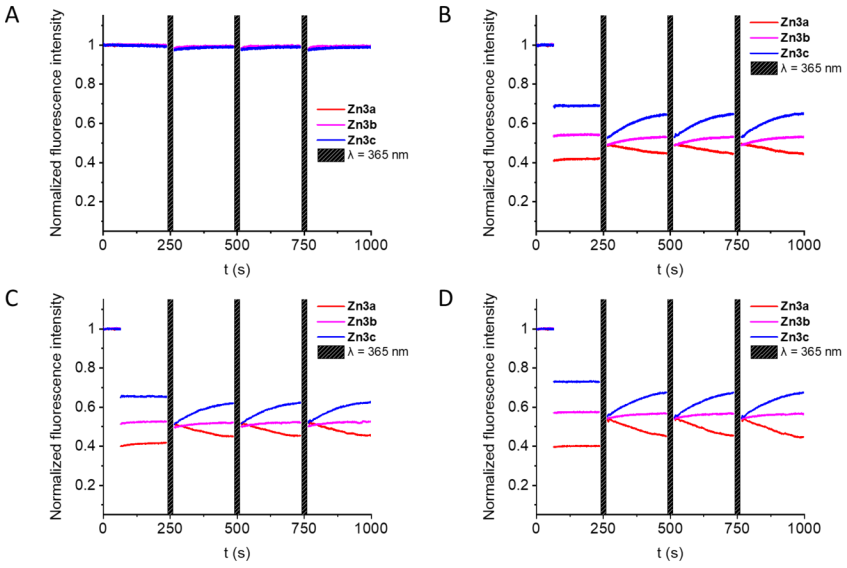

FIGURE 5 Normalized fluorescence intensities (λ_{ex} = 555 nm, λ_{em} = 657 nm, $CHCl_3/CH_3CN$, 1:1, v/v, 298 K) of the isomers of host **Zn3** as a function of time after the addition (at t = 50 s) of: (A) no guest, (B) 3.6 equivalents of guest**V4** , (C) 1.2 equivalents of guest **V5** , and (D) 13 equivalents of guest **V6** , and subsequent irradiation of the motor substituents (λ = 365 nm for 10 seconds) at t = 250, 500, 750 s, see bars.

effects of the photochemical isomerization of the motor substituents on the fluorescence emission of the zinc porphyrins. Figure 5A displays the normalized fluorescence intensity of all isomers of **Zn3** in the absence

of guest, with three intermediate irradiation events of 10 seconds (λ_{max} = 365 nm) at t = 250, 500, 750 s. These irradiation events turned out to not substantially change the fluorescence intensity of the zinc porphyrins of the hosts. Subsequently, we carried out the light-gated binding experiments. Figure 5B depicts the fluorescence intensities of the three isomeric hosts upon the addition of viologen guest **V4** (at t = 50 s, 3.6 equiv of guest was added). In all cases, an instant drop in fluorescence intensity indicated the formation of the host-guest complexes**Zn3·V4** , with host **Zn3a** having the highest host-guest occupancy, followed by **Zn3b** and then **Zn3c** . This trend is in line with the decrease in binding constant as determined by the fluorescence titrations (Table 1). The subsequent *in situ*photochemical isomerization of the motor substituents of **Zn3a**was associated with an instant increase in fluorescence intensity, indicating that the occupancy, and thus the binding affinity, dropped. Over time, thermal helix inversion of the motor substituents took place, resulting in the slow recovery of the original – higher – binding affinity. In sharp contrast, the photochemical isomerization of**Zn3c** resulted in an instant decrease in fluorescence intensity, which is associated with an increase in binding affinity. In analogy with the behavior of **Zn3a** , the thermal relaxation of the metastable motors regenerated the original – lower – binding affinity. For the non-symmetric host **Zn3b** , the effect of irradiation was the smallest. Only a small drop in fluorescence intensity was observed, which is in line with a small increase in binding affinity. This effect may be caused by differences in PSS ratios of the two non-identical motor substituents of **Zn3b** . If the bound motor has a higher PSS ratio than the loose motor, an increase in binding affinity is to be expected. Successive isomerization-THI cycles showed that the processes are repeatable for all isomers of **Zn3** (Figure 5B–D). In a next series of experiments, we evaluated the binding between the isomers of**Zn3** and benzyl viologen **V5** (Figure 5C), which has a higher affinity for the porphyrin cages compared to viologen guests**V4** and **V6** . The addition of a small excess of**V5** (at t = 50 s, 1.2 equiv of guest was added) to the solutions of the three isomers of **Zn3** caused a similar drop in fluorescence as was observed when 3.6 equiv of **V4** was added to the same hosts, highlighting the differences in binding affinity. Repeated isomerization-THI cycles indicated that the host-guest mixtures containing guest **V5** displayed similar light- and heat-responses as those containing guest **V4** . Finally, we examined whether the weakest binding viologen **V6** would also be susceptible to light-gated binding in the double-motorized porphyrin cages **Zn3**(Figure 5D). The addition of a large excess of **V6** (at t = 50 s, 13 equiv of guest was added) resulted in a similar decrease in fluorescence intensity as observed for **V4** (3.6 equiv) and**V5** (1.2 equiv). Again, the host-guest mixtures containing**V6** responded similarly to the photochemical isomerization-THI cycles as those containing **V4** and **V5** .

In summary, we have successfully synthesized light-responsive double-motorized porphyrin cage compounds **Zn3a** , **Zn3b** , and **Zn3c** . The structures and assignments of the absolute configurations of these compounds were established by 1D and 2D NMR, and by circular dichroism analysis. UV-vis and ^{1}H NMR analysis showed that cage compounds **Zn3** efficiently undergo photochemical isomerization and thermal helix inversion steps, in agreement with what we have shown previously for the single-motorized cage compounds **Zn2** .[30] Furthermore, the different stereoisomers of **Zn3** presented in this study show significant differences in binding affinity for viologen guests (K_a of **Zn3a** > **Zn3b**> **Zn3c**). These differences are attributed to differences in the three-dimensional structures of the isomeric hosts.**Zn3a** possesses two loosely bound motor fragments, whereas one of the motors of **Zn3b** and both motors of **Zn3c** display intramolecular supramolecular interactions with the cavity part of the hosts, which competes with viologen guest binding inside the porphyrin cage. Photochemical isomerization of the motor substituents leads to the unique phenomenon that two diastereomers can become pseudo-identical. This phenomenon leads to orthogonal behavior in light-gated binding of guest molecules. Whereas the photo-isomerization of the C_2-symmetric diastereomer **Zn3a** (two loose motors) significantly lowers its binding affinity for viologen guests, the opposite is true for the C_2-symmetric diastereomer **Zn3c** (two bound motors), i.e. its binding affinity increases. These studies show that a combination of fixed chiral elements, *e.g.* point chirality and planar chirality, with a light-responsive chiral element, *e.g.* helicity, gives rise to light-responsive functional molecular systems that can operate in an orthogonal fashion.

FUNDING

This work was funded by the European Research Council (ERC Advanced Grant No. 74092 to R.J.M.N. and

ERC Advanced Grant No. 227897 to B.L.F.) and by the Dutch Ministry of Education, Culture, and Science (Gravitation program 024.001.035).

CONFLICT OF INTEREST

The authors declare no conflict of interest.

DATA AVAILABILITY STATEMENT

The authors declare that the data supporting the findings of this study are available within the Supporting Information files and from the corresponding authors upon reasonable request.

ORCID

Roeland J. M. Nolte https://orcid.org/0000-0002-5612-7815

Johannes A. A. W. Elemans https://orcid.org/0000-0003-3825-7218

Ben L. Feringa https://orcid.org/0000-0003-0588-8435

Pieter J. Gilissen https://orcid.org/0000-0003-2111-9564

Nicolas Vanthuyne https://orcid.org/0000-0003-2598-7940

REFERENCES

1. Balzani V, Credi A, Raymo FM, Stoddart FJ. Artificial molecular machines. *Angew Chem Int Ed.* 2000;39:3348-3391.
2. Qu D-H, Wang Q-C, Zhang Q-W, Ma X, Tian H. Photoresponsive host-guest functional systems. *Chem Rev.* 2015;115:7543-7588.
3. Erbas-Cakmak S, Leigh DA, McTernan CT, Nussbaumer AL. Artificial molecular machines. *Chem Rev.* 2015;115:10081-10206.
4. Van Dijk L, Tilby MJ, Szpera R, Smith OA, Bunce HAP, Fletcher SP. Molecular machines for catalysis. *Nat Rev Chem.* 2018;2:0117.
5. Vlatković M, Collins BSL, Feringa BL. Dynamic responsive systems for catalytic function. *Chem Eur J.* 2016;22:17080-17111.
6. Blanco-Gómez A, Cortón P, Barravecchia L, Neira I, Pazos E, Peinador C, García MD. Controlled binding of organic guests by stimuli-responsive macrocycles. *Chem Soc Rev.*2020;49:3834-3862.
7. Bandara HMD, Burdette SC. Photoisomerization in different classes of azobenzene. *Chem Soc Rev.* 2012;41:1809-1825.
8. Waldeck DH. Photoisomerization dynamics of stilbenes. *Chem Rev.*1991;91:415-436.
9. Irie M. Diarylethenes for memories and switches. *Chem Rev.*2000;100:1685-1716.
10. Ueno A, Yoshimura H, Saka R, Osa T. Photocontrol of binding ability of capped cyclodextrin. *J Am Chem Soc.* 1979;101:2779-2780.
11. Muler A, Jukovic A, Van Leeuwen FWB, Kooijman H, Spek AL, Huskens J, Reinhoudt DN. Photocontrolled release and uptake of a porphyrin guest by dithienylethene-tethered β-cyclodextrin host dimers. *Chem Eur J.* 2004;10:1114-1123.
12. Takashima Y, Hatanaka S, Otsubo M, Nakahata M, Kakuta T, Hashidzume A, Yamaguchi H, Harada A. Expansion-contraction of photoresponsive artificial muscle regulated by host-guest interactions. *Nat Commun.* 2012;3:1270.
13. Cacciapaglia R, Di Stefano S, Mandolini L. The bis-barium complex of a butterfly crown ether as a phototunable supramolecular catalyst.*J Am Chem Soc.* 2003;125:2224-2227.
14. Cacciapaglia R, Di Stefano S, Mandolini L. Size-selective catalysis of ester and anilide cleavage by the dinuclear barium(II) complexes of*cis* - and *trans* -stilbenobis(18-crown-6). *J Org Chem.* 2002;67:521-525.

15. Xu J-F, Chen Y-Z, Wu L-Z, Tung C-H, Yang Q-Z. Synthesis of a photoresponsive cryptand and its complexations with paraquat and 2,7-diazapyrenium. *Org Lett.* 2014;16:684-687.
16. Ragazzon G, Baroncini M, Silvi S, Venturi M, Credi A. Light-powered autonomous and directional molecular motion of a dissipative self-assembling system. *Nat Nanotechnol.* 2015;10:70-75.
17. Dorel R, Miró C, Wei Y, Wezenberg SJ, Feringa BL. Cation-modulated rotary speed in a light-driven crown ether functionalized molecular motor. *Org Lett.* 2018;20:3715-3718.
18. Liu Y, Zhang Q, Crespi S, Chen S, Zhang XK, Xu T-Y, Ma C-S, Zhou S-Q, Shi Z-T, Tian H, Feringa BL, Qu D-H. Motorized macrocycle: a photo-responsive host with switchable and stereoselective guest recognition. *Angew Chem Int Ed.* 2021; doi.org/10.1002/anie.202104285.
19. García-López V, Liu D, Tour JM. Light-activated organic molecular motors and their applications. *Chem Rev.* 2020;120:79-124.
20. Koumura N, Zijlstra RWJ, Van Delden RA, Harada N, Feringa BL. Light-driven monodirectional molecular rotor. *Nature.*1999;401:152-155.
21. Koumura N, Geertsema EM, Van Gelder MB, Meetsma A, Feringa BL. Second generation light-driven molecular motors. Unidirectional rotation controlled by a single stereogenic center with near-perfect photoequilibria and acceleration of the speed of rotation by structural modification. *J Am Chem Soc.* 2002;124:5037-5051.
22. Pizzolato SF, Štacko P, Kistemaker JCM, Van Leeuwen T, Otten E, Feringa BL. Central-to-helical-to-axial-to-central transfer of chirality with a photoresponsive catalyst. *J Am Chem Soc.*2018;140:17278-17289.
23. Pizzolato SF, Štacko P, Kistemaker JCM, Van Leeuwen T, Feringa BL. Phosphoramidite-based photoresponsive ligands displaying multifold transfer of chirality in dynamic enantioselective metal catalysis.*Nat Catal.* 2020;3:488-496.
24. Elemans JAAW, Claase MB, Aarts PPM, Rowan AE, Schenning APHJ, Nolte RJM. Porphyrin clips derived from diphenylglycoluril. Synthesis, conformational analysis, and binding properties. *J Org Chem.*1999;64:7009-7016.
25. Gilissen PJ, White PB, Berrocal JA, Vanthuyne N, Rutjes FPJT, Feringa BL, Elemans JAAW, Nolte RJM. Molecular motor-functionalized porphyrin macrocycles. *Nat Commun.* 2020;11:5291.
26. Ouyang J, Swartjes A, Geerts M, Gilissen PJ, Wang D, Teeuwen PCP, Tinnemans P, Vanthuyne N, Chentouf S, Rutjes FPJT, Naubron J-V, Crassous J, Elemans JAAW, Nolte RJM. Absolute configuration and host-guest binding of chiral porphyrin-cages by a combined chiroptical and theoretical approach. *Nat Commun.* 2020;11:4776.
27. Vicario J, Meetsma A, Feringa BL. Controlling the speed of rotation in molecular motors. Dramatic acceleration of the rotary motion by structural modification. *Chem Commun.* 2005;5910-5912.